

# Assessing spatial coupling in complex population dynamics using mutual prediction and continuity statistics

J.M. Nichols<sup>a,\*</sup>, L. Moniz<sup>a</sup>, J.D. Nichols<sup>b</sup>, L.M. Pecora<sup>a</sup>, E. Cooch<sup>c</sup>

<sup>a</sup>*U.S. Naval Research Laboratory, Code 5673, 4555 Overlook Avenue, Washington, DC 20375, USA*

<sup>b</sup>*U.S. Geological Survey, Patuxent Wildlife Research Center, 11510 American Holly Drive, Laurel, MD 20708-4017, USA*

<sup>c</sup>*Department of Natural Resources, Cornell University, Ithaca, NY 14853, USA*

Received 8 January 2004

## Abstract

A number of important questions in ecology involve the possibility of interactions or “coupling” among potential components of ecological systems. The basic question of whether two components are coupled (exhibit dynamical interdependence) is relevant to investigations of movement of animals over space, population regulation, food webs and trophic interactions, and is also useful in the design of monitoring programs. For example, in spatially extended systems, coupling among populations in different locations implies the existence of redundant information in the system and the possibility of exploiting this redundancy in the development of spatial sampling designs. One approach to the identification of coupling involves study of the purported mechanisms linking system components. Another approach is based on time series of two potential components of the same system and, in previous ecological work, has relied on linear cross-correlation analysis. Here we present two different attractor-based approaches, continuity and mutual prediction, for determining the degree to which two population time series (e.g., at different spatial locations) are coupled. Both approaches are demonstrated on a one-dimensional predator–prey model system exhibiting complex dynamics. Of particular interest is the spatial asymmetry introduced into the model as linearly declining resource for the prey over the domain of the spatial coordinate. Results from these approaches are then compared to the more standard cross-correlation analysis. In contrast to cross-correlation, both continuity and mutual prediction are clearly able to discern the asymmetry in the flow of information through this system. Published by Elsevier Inc.

*Keywords:* Chaos; Mutual prediction; General synchrony; Attractor reconstruction; Continuity; Nonlinear systems

## 1. Introduction

Ecological systems and their constituent populations vary over time and space, and a central goal of ecologists is to develop mechanistic explanations for such variation that can be used for prediction (Rhodes et al., 1996; Ranta et al., 1997; Koenig, 1999; Bjørnstad and Grenfell, 2001; Keeling and Rohani, 2002). A class of mechanistic explanations of special interest to ecologists involves some kind of “coupling” (dynamical

interdependence) among system components. For single species populations in different locations, coupling usually requires movement among locations. This movement may involve changes in residence location (dispersal; Clobert et al., 2001) or regular shifts between seasonal residences (migration; Webster et al., 2002). For an ecological community in a single location, coupling among multiple species typically involves some sort of mechanistic ecological interaction such as competition (e.g., Durrett and Levin, 1998) or predation (e.g., Hastings, 2001; Tobin and Bjørnstad, 2003). For a community studied in multiple locations, coupling mechanisms can include both movement and interspecific interactions.

\*Corresponding author. Fax: +1 202 767 5792.

E-mail address: [pele@ccs.nrl.navy.mil](mailto:pele@ccs.nrl.navy.mil) (J.M. Nichols).

There are two general approaches to drawing inferences about coupling in ecological systems. One approach is to directly study the mechanisms themselves. For example, one might study movement of animals among different locations in a system of interest (e.g., Spendelov et al., 1995; Blums et al., 2003) or predation by one or more species on populations of prey (e.g., Karanth and Sunquist, 1995; Krebs et al., 1995; Korpimäki and Krebs, 1996). The other approach to the study of coupling is less direct and involves joint analyses of time-series data either from one or more species at multiple locations or from potentially interacting species at the same location(s) (Ranta et al., 1997; Koenig, 1999; Bjørnstad et al., 1999a, b; Bjørnstad and Grenfell, 2001; Tobin and Bjørnstad, 2003). In this paper, we focus on the second approach and on efforts to detect coupling between two potentially interacting systems based on time series of state variables characterizing system dynamics.

Assume that we have measured state variables such as population size at two nearby locations over a large number of years or generations or other time intervals of interest. From these data, we would like to draw inferences about the existence, strength, and even direction of possible coupling of the populations and their associated dynamics (which are needed to both parsimoniously specify the current state of the system, but also to predict expected system change). The traditional approach of ecologists to such inferences focuses on spatial covariance in population dynamics and uses cross-correlation, typically with time lag 0 (Ranta et al., 1997; Bjørnstad et al., 1999a, b; Koenig, 1999; Keeling and Rohani, 2002; Post and Forchhammer, 2002). Specifically, the Pearson product-moment correlation coefficient is computed between either population sizes or rates of change in population size (ratios of abundance in successive sampling periods) in the two locations. Use of rates of population change, rather than population size itself, is intended to exclude correlations that might arise from simple time trends in abundance. Positive correlations resulting from such analyses are interpreted as evidence of, and sometimes even used to define, population synchrony (Post and Forchhammer, 2002). In addition, moment closure methods have been suggested for accommodating higher-order correlation densities, which may provide a better description of system dynamics in some cases (Dieckmann et al., 2000).

Cross-correlation is based on linear measures and addresses the existence of a specific kind of functional relationship between time series. For linear systems, cross-correlation is adequate to detect and describe dynamical interdependence of pairs of system state variables, where “dynamical interdependence” essentially means that the state variables are both components of the same dynamical system (e.g., Schiff et al.,

1996). However, small linear correlation does not imply that other (nonlinear) functional relationships do not exist (Pecora et al., 1995). The nonlinear dynamics that characterize at least some biological populations and communities (Schaffer, 1985; Schaffer and Kot, 1986; Constantino et al., 1995, 1997; Dennis et al., 1995, 1997) argue for the use of a more general approach to assessment of dynamical interdependence.

Another limitation of linear cross-correlation is the symmetric nature of the function. The influence of the dynamics of one component of an ecological system on the dynamics of another component, and hence the flow of information in such a system, are frequently asymmetric. For example, in the strict source–sink system described by Pulliam (1988), the source population is not influenced by dynamics of animals in the sink, whereas sink dynamics are largely determined by dynamics of the source population. Linkages among food web components are frequently asymmetric, and the concepts of top-down vs. bottom-up regulation (e.g., Harrison and Cappuccino, 1995) are based on such asymmetries. Monitoring programs for ecosystems frequently are based on the concept of “indicator species”. This concept is based on the premise that dynamics of some system components carry more information about the system than dynamics of other components. Identification of such asymmetries in information content is important to the design of monitoring programs. General methods able to identify asymmetries in influence or information flow among system components would thus be useful to ecologists.

A more general approach than looking for a specific (e.g., linear) functional relationship between two time series involves first reconstructing the dynamics of the two systems, for example using attractor reconstruction via delay coordinates (Sauer et al., 1991; Williams, 1997; Kantz and Schreiber, 1999), and then generally asking whether the attractors are related by a function. Takens’ embedding theorem (Takens, 1981) states that the trajectory of a dynamical system in phase space can be reconstructed from a time series of a single state variable from the system. Thus, a functional relationship must exist between attractors reconstructed from different state variables from the same system. The possibility of dynamical interdependence can be investigated by drawing inferences about the properties of potential functions relating two reconstructed attractors. In this paper, we use two approaches to this type of inference, *mutual prediction* (Schiff et al., 1996) and *continuity statistics* (Pecora et al., 1995; Pecora and Carroll, 1996; Moniz et al., 2004).

Continuity tests for the existence of a mapping from one time series to another i.e. does a functional relationship exist? This same test, applied in reverse, can test for the mathematical concept of injectivity, i.e. points that are close together in the second time series

are also close together in the first. Mathematical definitions of continuity, injectivity and the practical implementation of this test are discussed in Section 2.3. Given that a relationship exists, one can determine the degree to which one time series predicts the other. In fact, measures of predictability have been used as a test of continuity between time series-data (Schiff et al., 1996). Certainly, if one time series can predict the other, the two are related by *some* function. The concept of mutual predictability is discussed in Section 2.4. Both tests are then applied to data collected from a spatially extended predator–prey model exhibiting complex dynamics and used to determine the degree of coupling between spatially extended time series. Comparisons are made between continuity, mutual prediction, and the more standard approach of using cross-correlation in order to quantify the degree of coupling. Results highlight the clear inability of the cross-correlation function to extract the relevant, and in this case asymmetric, dynamical relationships between ecological time series. Results also indicate the subtle yet important differences between continuity and mutual prediction. Although they are ostensibly measuring the same thing the implementation can lead to non-trivial differences in the information they provide. In light of these important differences these two metrics should be viewed as complementary to each other rather than as alternatives.

## 2. Time-series analysis for inference about coupling

### 2.1. Cross-correlation analysis

The standard approach of ecologists for assessing the degree of coupling between time series at different spatial locations is the cross-correlation function. Given two time series,  $x(n)$  and  $y(n)$ , the linear cross-correlation is computed via the cross-covariance,

$$c_{xy}(k) = \frac{1}{N-k} \sum_{i=1}^{N-k} (x(i) - \bar{x})(y(i+k) - \bar{y}),$$

$$k = 0, 1, 2, \dots \tag{1}$$

as

$$r_{xy}(k) = \frac{c_{xy}(k)}{\frac{1}{N-k} \sqrt{\sum_{i=1}^{N-k} (x(i) - \bar{x})^2 \sum_{i=1}^{N-k} (y(i) - \bar{y})^2}}. \tag{2}$$

Cross-correlation values for negative lags may be obtained by noting that  $r_{xy}(-k) = r_{yx}(k)$ . By design, this particular metric is testing for the presence of a linear functional relationship between the dynamics of  $x$  and  $y$ . Values near unity are strong indicators that such a relationship exists while those near zero imply the absence of coupling. The cross-correlation function will

typically fluctuate as a function of delay (phase)  $k$ . It is therefore convenient to quantify the coupling strength by taking the maximum of Eq. (2):

$$\gamma_{xy}^R = \max |r_{xy}(k)|, \quad k = 1, \dots, N, \tag{3}$$

where the superscript  $R$  will be used to denote “cross-correlation”. This particular metric is the current standard in ecological investigations and has been used in a variety of applications (e.g., Bjørnstad et al., 1999a, b; Koenig, 1999; Post and Forchhammer, 2002).

### 2.2. Attractor-based methods: review of phase space analysis

The other two approaches to inference about coupling, continuity and mutual prediction, are based on phase space analysis and attractor reconstruction. Assume the dynamics of a system evolve according to  $\dot{\mathbf{x}}(t) = \mathbf{F}(\mathbf{x}(t))$ ,  $\mathbf{x} \in \mathbb{R}^d$ . An alternative to time or frequency domain descriptions of the dynamics is to view the system output in the  $d$ -dimensional space defined by the state variables  $\mathbf{x}$ , or, phase space. An initial condition  $\mathbf{x}(0)$  will, under the action of  $\mathbf{F}$ , asymptotically approach a subset of phase space referred to as the system’s attractor  $X$ . The attractor may be thought of as a geometric object (a collection of points) in phase space to which a set of nearby trajectories approaches. In practice, one simply plots the measured variables against each other and then uses the resulting steady state, geometric portrait of the dynamics to describe the system. For example, the attractor for the well-known two-dimensional Lotka–Volterra predator/prey model is visualized by plotting predator vs. prey ( $x_1$  vs.  $x_2$ ). A variety of attractor-based metrics exist for quantifying various aspects of system dynamics, and these metrics have seen some use in ecology (Schaffer, 1985; Schaffer and Kot, 1986; Hastings et al., 1993; Pascual, 1993; Little et al., 1996; Pascual and Levin, 1999; Pascual and Ellner, 2000).

For certain systems the practitioner may be unable to measure, or even identify, each of the system’s state variables. In this case we make use of a collection of powerful mathematical theorems referred to collectively as the *embedding theorems*. The theorems are generally credited to the early work of Whitney (1936) and later Takens (1981) and have been generalized in subsequent work by Sauer et al. (1991), and more recently, Ott and Yorke (2003). Using a single measure of system response (time-series of a single state variable), the complete state vector may be *qualitatively* reconstructed at any point in time via

$$\mathbf{X} \equiv \mathbf{x}(n) = (x(n), x(n+T), \dots, x(n+(m-1)T)). \tag{4}$$

Here boldface type denotes a vector and the uppercase  $X$  is used to represent the entire ensemble of points comprising the attractor. The reconstructed

pseudo-state vectors are simply delayed copies of the original time series and will qualitatively preserve the dynamics of the “true” underlying system provided that the delay  $T$  and embedding dimension  $m$  are chosen properly. Suggestions for these choices are given by Fraser and Swinney (1986) and Kantz and Schreiber (1999) for delay and Kennel et al. (1992) for embedding dimension.

2.3. *Attractor-based methods: continuity*

Continuity of a function  $f$  at point  $x_0$  in a domain  $X$  implies that for every neighborhood  $V$  of  $f(x_0)$  there must exist a neighborhood  $U$  around  $x_0$  such that all points within  $U$  map into  $V$ . The precise mathematical definition is as follows: for every  $x_0 \in X, \forall \varepsilon > 0 \exists \delta > 0$  such that  $\|x - x_0\| < \delta \rightarrow \|f(x) - f(x_0)\| < \varepsilon$ . In other words, for a given set  $V$  of points in a local region of size  $\varepsilon$  on the  $f(X)$  attractor, there is a corresponding  $\delta$ -sized set  $U$  on the  $X$  attractor from which points in  $V$  originated. A schematic illustrating the concept of continuity is shown in Fig. 1 (left). Points within the  $\delta$ -ball on the “source” attractor are mapped via the function  $F$  into an  $\varepsilon$ -ball on the second “target” attractor. A lack of continuity is therefore indicated by points in the  $\delta$ -ball failing to map into the  $\varepsilon$ -ball (Fig. 1, center). If a function between source and target is indicated but the inverse relationship is *not*, this indicates that the population in the target region depends on the source, but the source does not depend on the target. Typically, this means that dynamics in the source are somehow collapsed onto the target by the function. The situation where  $F^{-1}$  fails to be continuous is depicted in Fig. 1(right).

Assuming for now that the data do not include noise, implementing the definition algorithmically is straightforward. In the context of spatially distributed systems we are searching for the existence of the function  $f$  between data collected from two different spatial locations. We begin with two  $N$ -point attractors  $\mathbf{x}(n)$  and  $\mathbf{y}(n), n = 1, \dots, N$  either measured directly or reconstructed using Eq. (4). These two attractors will

be referred to as the “source” and “target”, respectively. A fiducial point is chosen randomly from the source as  $\mathbf{x}(f)$  and the near neighbors located as  $\mathbf{x}(p_i) : \|\mathbf{x}(p_i) - \mathbf{x}(f)\| < \delta, i = 1, \dots, n_\delta$ . The corresponding neighborhood on the target attractor is given by the points with the same time indices,  $\mathbf{y}(p_i)$ . We then check to see if  $\|\mathbf{y}(p_i) - \mathbf{y}(f)\| < \varepsilon$ , denoting the number of points that meet this criteria  $n_\varepsilon$ . Of course, not all points will map into the  $\varepsilon$  neighborhood even if there is continuity between the two data sets. If a point in the source neighborhood is present due to noise (e.g., measurement error), that point will most likely not map into the target neighborhood. Making the algorithm practical therefore requires making a probabilistic judgment with respect to how many points from the  $\delta$  region are required to map to the  $\varepsilon$  region.

We establish a relevant null hypothesis by assuming that points from the given  $\delta$ -ball map to points in the  $\varepsilon$ -ball by a coin flip. In order to reject the null (equivalently, to *accept* the  $\delta$ -ball as passing the continuity test for this  $\varepsilon$ ), we must lie in the tail of the binomial distribution. Thus, we must have 95% confidence that the points from the  $\delta$ -ball did *not* map to the  $\varepsilon$ -ball by guessing. To quantify this, the probability of each  $x$  in the  $\delta$ -ball mapping *inside* the  $\varepsilon$ -ball is 0.5. Then for  $n_\delta$  points in the  $\delta$  ball, we find the number  $n_\varepsilon$  of corresponding points in the  $\varepsilon$  ball. The null hypothesis is rejected with 95% confidence for this  $\varepsilon$  if

$$\sum_{j=n_\varepsilon}^{n_\delta} \binom{n_\delta}{j} (0.5)^j (0.5)^{n_\delta-j} < 0.05, \tag{5}$$

that is, if the probability of having  $n_\varepsilon$  or more of the  $n_\delta$   $\delta$ -ball points land in the  $\varepsilon$ -ball by chance is less than 0.05. We formulate the statistic to be based not on the acceptance or rejection of the null hypothesis, but on the *minimum*  $\varepsilon$  that can be used to reject the null hypothesis at each point. We call this value  $\varepsilon^*$ . This is the smallest  $\varepsilon$  for which a  $\delta$  can be found to reject the null hypothesis.

We perform this computation about some number of fiducial points  $N_f$  and take the average value as the

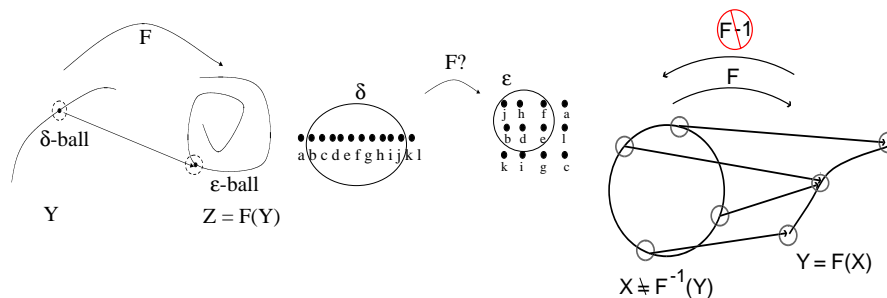


Fig. 1. Illustration of the existence of a continuous function between source and target attractors (left), the absence of such a function resulting in points from  $\delta$ -balls that do not all map to the  $\varepsilon$ -ball (middle), and A continuous function with no continuous inverse i.e. points from the  $\varepsilon$ -ball have preimages in 2 disjoint  $\delta$ -balls and no continuity between hypothetical attractors (right).

measure reflecting continuity between the data  $X$  and  $Y$  via

$$\gamma_{xy}^C = \frac{1}{N_f} \sum_f^{N_f} \varepsilon_f^* \tag{6}$$

where superscript  $C$  denotes “continuity”. The continuity statistic for known functional relationships, e.g., between one spatial location and itself, provides the baseline  $\gamma_{xx}^C$ . Values of  $\gamma_{xy}^C$  for other proposed relationships are then computed and compared to this baseline to suggest existence or non-existence of a functional relationship between the source and the target. Note that this is a one-way statistic; the existence of a function from source to target does not guarantee the existence of a continuous function from target to source. The continuity of an inverse function can be tested by reversing source and target and finding  $\varepsilon^*$ ’s for the proposed inverse function (see again Fig. 1 right). This property is what allows the continuity metric to expose asymmetries in the data.

#### 2.4. Attractor-based methods: mutual prediction

The mutual prediction algorithm assesses the degree to which the dynamics of one signal or attractor can be used to predict the dynamics of another. If one set of data can accurately forecast points on the other set, the two systems are assumed to be coupled in some fashion implying dynamical interdependence. The mutual prediction algorithm has also been used to establish continuity between time series Schiff et al. (1996); yet is different from the above described continuity test in a very important way (to be described). These two

algorithms, continuity and mutual prediction, should therefore be viewed not as competing metrics for assessing continuity, but instead as alternatives for establishing the existence of a functional relationship between time series.

As with the continuity metric, let  $\mathbf{x}(n)$  be the attractor at location 1 and  $\mathbf{y}(n)$  be the attractor at location 2. We wish to see the degree to which the dynamical description at location 1 can be used to forecast values on the attractor at location 2. A fiducial trajectory (i.e. a point) is randomly selected on attractor 2 as  $\mathbf{y}(f)$ . The neighborhood local to this point is then selected from the attractor at location 1 as  $\mathbf{x}(p_i) : \|\mathbf{x}(p_i) - \mathbf{y}(f)\| < \varepsilon, i = 1, \dots, n_\varepsilon$ . Note the time indices  $p_i$  need not have any temporal relationship to the fiducial point, as the selection of the neighborhood is made using only geometric considerations. This local neighborhood can then be used to make the  $s$ -step forecast

$$\hat{\mathbf{y}}(f + s) = \frac{1}{n_\varepsilon} \sum_{i=1}^{n_\varepsilon} \mathbf{x}(p_i + s). \tag{7}$$

Eq. (7) makes a zeroth-order prediction of the dynamics at location 2 using the description at location 1. In this work we use a prediction horizon of  $s = 1$ . A measure of dynamical dissimilarity is then introduced as

$$\gamma_{xy}^M = \frac{1}{m\sigma_x^2} \|\hat{\mathbf{y}}(f + s) - \mathbf{y}(f + s)\|, \tag{8}$$

where the normalizing constant is the variance of the first time series,  $\sigma_x^2 = 1/(N - 1) \sum_{n=1}^N (x(n) - \bar{x})^2$  (overbar denotes mean) multiplied by the dimension of the attractor. Because the prediction is made in  $m$  dimensions the error is resolved with the operator  $\|\cdot\|$  which takes the Euclidean distance between observed and

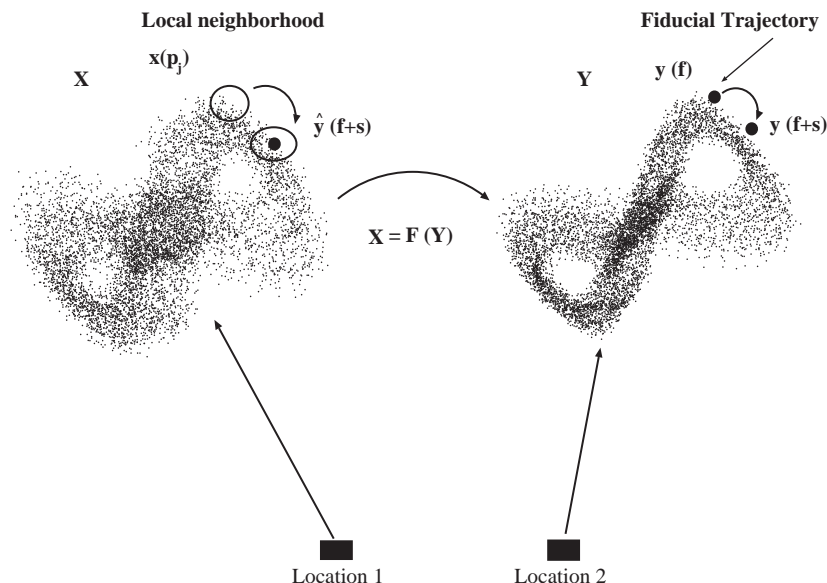


Fig. 2. Description of mutual prediction algorithm.

predicted values. An illustration of the algorithm is provided in Fig. 2 where the attractor at location 1 is used to forecast points on location 2. Similar dynamics result in low prediction errors while errors close to unity occur for two dissimilar processes.

Implementation of this scheme requires both a choice of  $\varepsilon$  and a mechanism for dealing with sparsely populated neighborhoods. With regard to the latter, if no near neighbors can be found, the best possible prediction is to choose the mean of the time series as the future value i.e.  $\hat{y}(f+s) = \bar{x}(n)$ . Choice of  $\varepsilon$  is typically made such that the neighborhoods reflect local dynamics, yet are large enough so that a sufficient number of points (on average) can be found in the neighborhoods. A convenient rule of thumb, used by the authors and others, is to choose  $0.01\sigma < \varepsilon < 0.1\sigma$ , where  $\sigma$  is the standard deviation of the time series.

Mutual prediction is different from continuity in that the neighborhoods being compared are established through purely geometric considerations (as opposed to using the same time indices when establishing neighborhoods in continuity). It is therefore entirely possible to have excellent continuity and large prediction errors. Even for small  $\varepsilon^*$  if there exist no near neighbors on  $\mathbf{x}(n)$  (in a geometric sense) to the fiducial point  $\mathbf{y}(f)$ , the prediction will be poor. Likewise, there can exist poor continuity and small prediction errors. Again, dynamics that evolve in similar fashion at similar attractor locations are all that is required for good predictability whereas good continuity requires *temporally* associated neighborhoods to remain local (i.e. have a small  $\varepsilon^*$ ). In many situations, however, these two metrics tend to produce similar results and both can be used effectively to assess the directionality of information flow in nonlinear, spatially extended systems.

### 3. Numerical model

In order to contrast the three approaches to assessment of coupling, a spatially one-dimensional predator–prey model was considered. The model was introduced by Pascual (1993) and explored further by Little et al. (1996) and describes the evolution of the prey  $p$  and predator  $h$  according to

$$\begin{aligned} \frac{\partial p}{\partial t} &= r_x p(1-p) - \frac{ap}{1+bp} h + d \frac{\partial^2 p}{\partial x^2}, \\ \frac{\partial h}{\partial t} &= \frac{ap}{1+bp} h - mh + d \frac{\partial^2 h}{\partial x^2}, \\ r_x &= e - fx. \end{aligned} \quad (9)$$

The dimensionless variables  $p, h$ , and  $x$  represent the prey density, predator density, and spatial coordinate, respectively. Reflective boundary conditions are considered at  $x = 0, 1$  as  $\frac{\partial p}{\partial x} = \frac{\partial h}{\partial x} = 0$ . Parameters are the

predator death rate,  $m$ , diffusion coefficient  $d$ , the predator/prey coupling  $a$ , the prey carrying capacity  $b$ , and the intrinsic growth rate  $r_x$  of the prey population, which is (for non-zero  $f$ ) a function of space. The resource term is a linearly declining function of space with value  $r_0 = e = \text{const.}$  at the boundary. The parameter  $f$  governs the rate of resource decline and hence the degree of spatial asymmetry. As in Pascual (1993) the death rate, diffusion coefficient, boundary resource, and carrying capacity are fixed at  $m = 0.6$ ,  $d = 10^{-4}$ ,  $e = 5.0$ ,  $b = 2.0$ .

In the absence of diffusion, this system possesses three fixed point (equilibrium) solutions

$$\text{FP}^{1,2,3} \equiv (p^*, h^*) = \left[ (0, 0), (1, 0), \left( \frac{m}{a - mb}, \frac{a - (1 + b)m(e - fx)}{(a - bm)^2} \right) \right].$$

The stability of these equilibria is largely governed by the coupling coefficient  $a$ . The eigenvalues  $\lambda$  of the Jacobian of Eq. (9) evaluated at  $\text{FP}^{2,3}$  ( $\text{FP}^1$  is the trivial solution) give the following results. For  $a < 3.6$  the stable solution is given by  $\text{FP}^2 = (1, 0)$  at every point in space. For  $a \geq 3.6$  this point becomes universally (for all  $x$ ) unstable and all trajectories at all spatial locations migrate toward  $\text{FP}^3$ . This new solution remains stable for  $3.6 \leq a \leq 4.5$ , however the *type* of stability varies as a function of  $x$ . As  $a$  is increased the eigenvalues of the Jacobian begin taking on imaginary parts. In the case of  $f = 1.9$ , for example, perturbations to  $\text{FP}^3$  for  $3.65 \leq a \leq 3.95$  progress from exponential decay to oscillatory decay in a cascade starting at  $x = 1$  as the imaginary parts of  $\lambda$  become positive (see Fig. 3c). Then, for  $a = 4.5$  each of the lattice sites simultaneously (independent of  $x$ ) undergoes a Hopf bifurcation with the oscillations occurring at different frequencies, dictated by the imaginary parts of the eigenvalues. Fig. 3d shows the variations in  $\text{Im}(\lambda)$  with  $x$  for three different values of resource slope. The steeper the slope in the resource term, the more disparate the frequencies of oscillation as the location is changed from  $x = 0$  to 1. The interplay between variations in frequency with  $x$ , and the coupling made possible by the addition of the diffusive term are most likely necessary for complex dynamics. Earlier work on this model (Pascual, 1993) showed that for  $d = 10^{-4}$  the system in fact does exhibit chaos.

Fig. 4 illustrates the effect of changing the slope  $f$  on the resulting phase plots of  $p$  vs.  $h$ . Clearly, the dynamics are more complex near  $x = 1$  as the presence of multiple frequency components are visible in the attractors. This is in contrast to the attractors at  $x = 0$  which exhibit only a single-frequency limit cycle oscillation. One possible reason for the asymmetry concerns the average number of predators as a function of space. From the

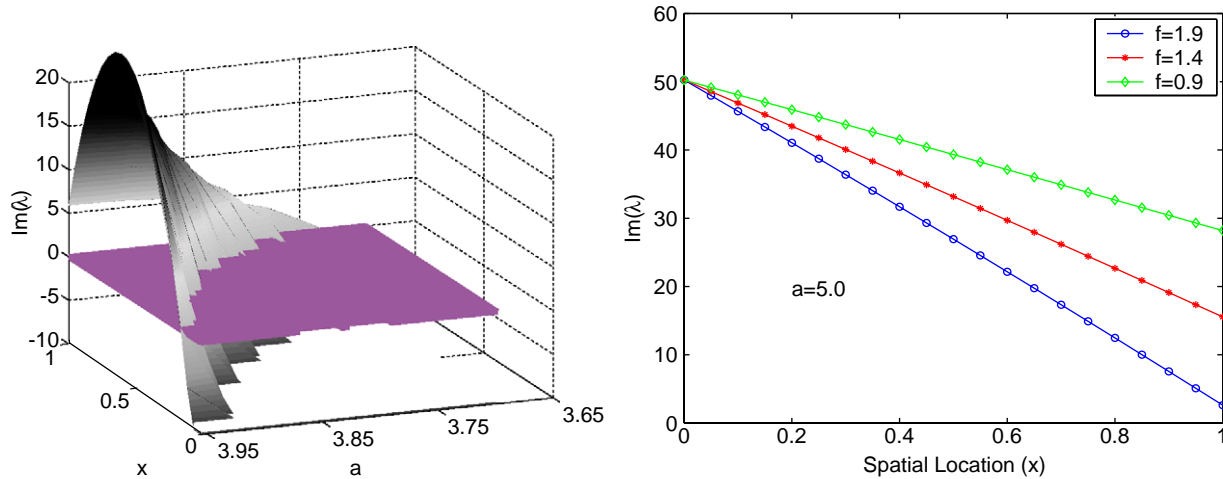


Fig. 3. Cascade transition to oscillatory behavior as a function of “*a*” (left) and differences in linearized frequencies as a function of “*x*” for varying resource gradients (right).

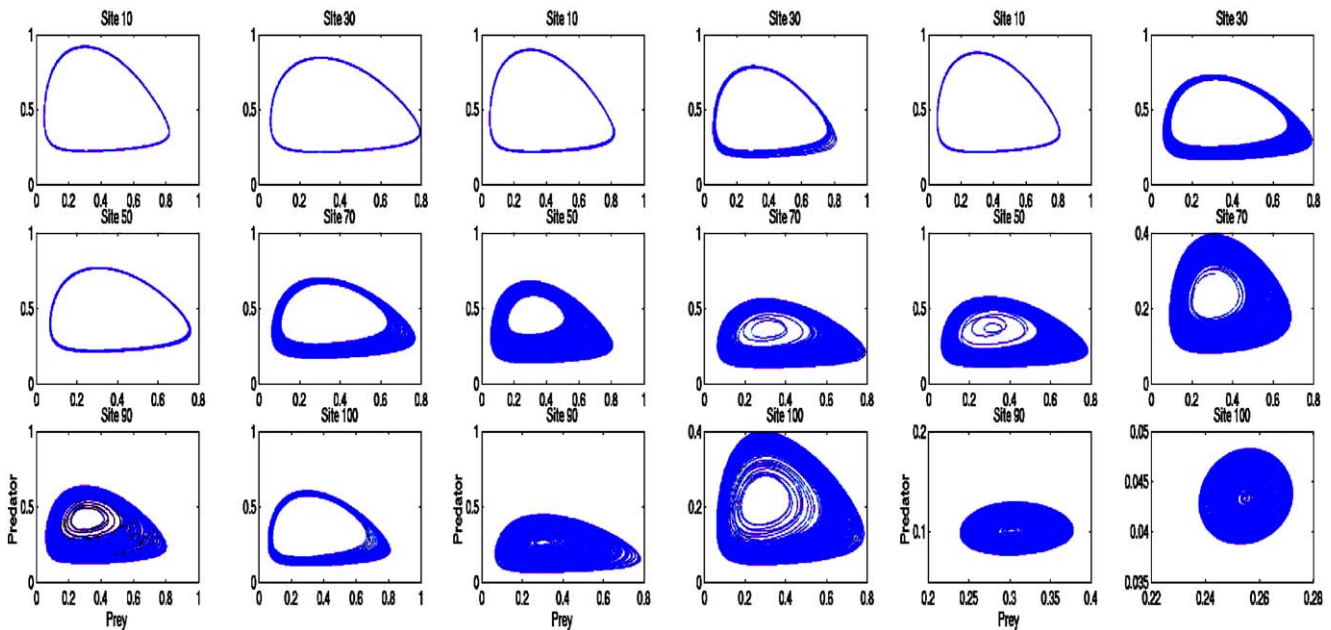


Fig. 4. Attractors (p v. h) at varying spatial locations for  $f = 0.9$  (left two columns), 1.4 (center columns), 1.9 (right two columns).

fixed-point analysis,  $FP^3$  is a linearly decreasing function of  $x$  for the predator term (this is also evidenced in the attractors of Fig. 4). Therefore, far fewer predators exist, on average, near  $x = 1$ . This is important when considering the coupling term  $d(\partial^2 h / \partial x^2)$ . By numerical approximation this term is given by  $(d/\Delta x^2)(h_{i+1} - 2h_i + h_{i-1})$ , where  $\Delta x$  is the spatial resolution and the notation  $h_i$  denotes the predator population at the  $i$ th lattice site. If the number of predators is larger at site  $i - 1$ , the dynamics at that site will have a larger influence on the dynamics at site  $i$  than will those at site  $i + 1$ . By this mechanism, information at

lower spatial indices (higher resource abundance) can more easily influence the dynamics at higher indices (lower resource abundance). The dynamics near  $x = 1$  therefore show an increased complexity as those sites are influenced by all other sites for  $x < 1$ . Within-site processes should be more important to the dynamics of high-resource sites (small  $x$ ), whereas immigration from other locations are expected to be more important to the dynamics of low-resource sites (large  $x$ ). As a result, dynamical information tends to propagate “downhill” toward regions of low-resource abundance.

#### 4. Application of approaches to assessment of coupling

We sought to use the spatial predator–prey model to investigate the three described approaches to assessment of coupling. Specifically, predator and prey dynamics throughout the spatial system are coupled via predator–prey interactions and movement. Thus, we can assess the evidence of coupling, for example, between predator and prey dynamics at the same or any other site. We expected the two attractor-based approaches to be perhaps more sensitive to coupling, as they are appropriate for use with nonlinear systems, whereas cross-correlation is not guaranteed to work well with such systems. As discussed above, we also expected the system to exhibit an asymmetric flow of information, which we expected to be detectable with the two attractor-based methods and not with cross-correlation.

Using a finite difference scheme, Eqs. (9) were integrated for  $N = 10,000$  time steps (post-transient) with a dimensionless sampling time of 0.5. The dominant frequency for this system is  $\approx 0.065$  cycles per unit time so that this sampling rate was deemed sufficient to capture the dynamics. Simulations were performed on a spatial grid consisting of 100 sites, distributed evenly on  $x \in [0, 1]$ . Three different resource slopes were used  $f = 0.9, 1.4, 1.9$  in order to study the effects of the resource gradient on the resulting spatial coupling. Prior to the analysis all time series were normalized by subtracting their mean and dividing by the standard deviation. Simple changes in population mean and/or variance are therefore removed from consideration here. The analysis of coupling focused on the relationship between predator/prey density at one site and predator/prey density at the same or another site. The attractor at a given location  $x$  may therefore be defined in terms of the predator and prey populations at that site as  $X = ((p_x(n), h_x(n)), n = 1, \dots, N$ .

For each of the approaches described in Section 2, comparisons were made using data recorded at locations  $x = 0.01, 0.05, \dots, 1.0$  resulting in the  $20 \times 20$  cross-correlation, continuity and mutual prediction matrices  $\gamma_{xx'}^R, \gamma_{xx'}^C, \gamma_{xx'}^M, x, x' \in [0, 1]$ . In an effort to place the three metrics on the same general scale, we take  $1.0 - \gamma_{xx'}^R$  as the measure of cross-correlation. Under this transformation, continuity, mutual prediction and cross-correlation metrics near zero indicate strong coupling, whereas values near unity are indicative of weak coupling.

Fig. 5 shows the cross-correlation, continuity, and mutual prediction statistics reflecting coupling between the data for predator/prey density at one site and predator/prey density at another site. All metrics show the strongest evidence of coupling on the diagonal, as expected. Population dynamics at nearby locations are more likely to be strongly coupled than those with a large separation. As the pair of sites being analyzed become more distant, all measures show a degradation

in the coupling. However, unlike correlation, continuity and prediction error clearly show the asymmetry associated with the flow of animals and information along the resource gradient. For the  $f = 0.9$  case the system dynamics are strongly coupled over most distances. The dynamics at most of the lattice sites are confined to near-periodic behavior as illustrated in Fig. 4, resulting in strong continuity and predictability. Continuity strongly resembles autocorrelation but is clearly capable of resolving differences in the coupling direction. Source values taken near the high-resource end of the system ( $x = 0$ ) tend to require large  $\varepsilon^*$  values when being compared with time series at the low-resource end ( $x = 1$ ). However, reversing the source/target relationship reveals a different pattern. Taking source values near  $x = 1$  shows stronger continuity when compared to targets at the high-resource end. Cross-correlation, on the other hand, cannot by definition resolve these differences. Results obtained using mutual prediction show similar asymmetries with one important difference. Comparing extremely low vs. extremely high lattice sites can actually result in excellent mutual predictability. Again this can be seen in part by analyzing the attractors observed at these sites. Due to the boundary conditions, attractors near  $x = 0$  and 1 possess similar geometry, hence, tend to have good mutual predictability. Results using the mutual prediction algorithm were based on  $\varepsilon = 0.025$  however we note that similar results were obtained for  $\varepsilon$  in the range  $0.01 \leq \varepsilon \leq 0.1$ .

Results for the  $f = 1.4$  resource gradient are shown in the second column. These data correspond to the gradient analyzed in Pascual's original paper using this model (Pascual, 1993). For all metrics used the region of strong coupling decreases relative to the previous gradient. Essentially a steeper resource gradient will result in more dissimilar dynamics across the lattice sites. Again, continuity and mutual prediction detect the effects of the gradient. Both continuity and mutual prediction indicate a stronger coupling examining the relationship from low-resource to high-resource areas then in going from high to low. This is consistent with results for  $f = 0.9$ . This particular directionality implies that dynamics nearer the high-resource end have a greater effect on those at the low-resource end than vice versa. Essentially, the gradient results in higher populations at the high-resource end. Consequently, through the nature of diffusive coupling (alluded to in Section 3), those dynamics have more influence on those occurring at sites with smaller (on average) populations. Conversely, dynamics at high-resource sites are not strongly influenced by movement from low-resource sites. For the most part, continuity and mutual prediction show similar features with one notable exceptions. Results based on mutual prediction show much sharper gradients in transitioning from regions of low to high

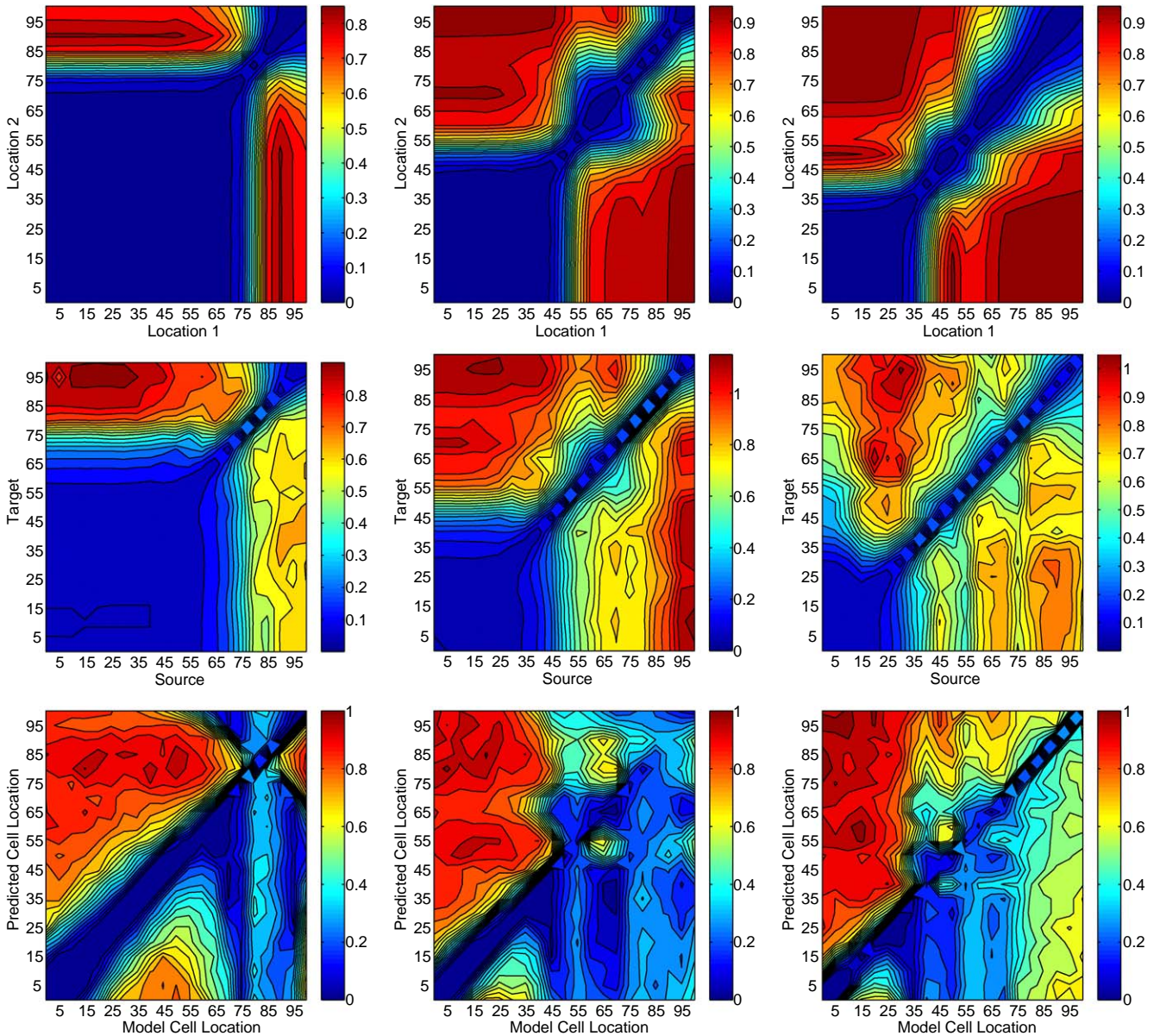


Fig. 5. Top row: cross-correlation  $(1.0 - \gamma_{xx})$ , middle row: continuity, and bottom row: Mutual prediction for  $f = 0.9, 1.4, 1.9$ .

predictability. This is a result of the way in which “sparse” neighborhoods are dealt with. By predicting the mean when no near neighbors are found, the transition from similar to dissimilar geometries is sudden in terms of the resulting prediction error.

The final set of observations corresponds to  $f = 1.9$ . Again, there exists a stronger functional relationship in the direction of decreasing resource than in the other direction. Both continuity and mutual prediction show very pronounced asymmetries in the coupling direction. Information about sites near  $x = 0$  is available to sites near  $x = 1$ , but not vice versa. Therefore, sites near  $x = 1$  possess more of the global system information and can therefore more accurately describe distant dynamics. The reverse is not true. The dynamics at sites near  $x = 0$

are influenced to a much lesser degree by the dynamics at other locations and therefore fail in trying to describe those dynamics. The cross-correlation metric is unable to detect the asymmetry and shows identical correlations regardless of which site is considered the “base” site. The correlation coefficient gives what is essentially the worst-case scenario. Because of the symmetry in the computation of this coefficient, regions of poor *uni*-directional coupling will appear as regions of poor *bi*-directional coupling.

One useful property of the correlation analysis as presented here, however, is that it only requires one of the state variables (in this case we used  $p$ ) to be recorded. The attractor-based approaches, on the other hand, involve measurements of both prey and predator

dynamics to form the attractors at the various lattice sites. This could conceivably give cross-correlation a practical advantage in such an analysis. However, according to the embedding theorems, measurements of a single variable can be used to qualitatively reconstruct the other provided that they are somehow coupled through common system dynamics. In this case the coupling is explicitly dictated by the parameter “ $a$ ”. In order to illustrate the utility of attractor-based approaches for meta-population systems in which animals at different sites are coupled through movements of individuals of the same species, we repeated the mutual prediction and continuity algorithms using only the observation  $p(n)$  to form the attractor

$$X = (p(n), p(n + T), p(n + 2T)),$$

where the optimal delay was chosen based on the mutual information function as  $T = 7$  time steps. The embedding dimension was chosen as  $m = 3$  based on the aforementioned false-nearest neighbors algorithm. Results using the attractor reconstruction for  $f = 1.4$  are shown in Fig. 6 for both mutual prediction and the continuity statistic. These results are similar to those found using both observations of  $p$  and  $h$  to form the attractors. The continuity metric gives nearly identical results using the delay coordinate approach as it does when one has access to each of the state variables. The one apparent difference is that using delay coordinates, the magnitude of the continuity metric increases. This can be explained in terms of the number of data,  $N$ , in the recorded time series. In the previous approach we had access to  $N = 10,000$  points for each of the two

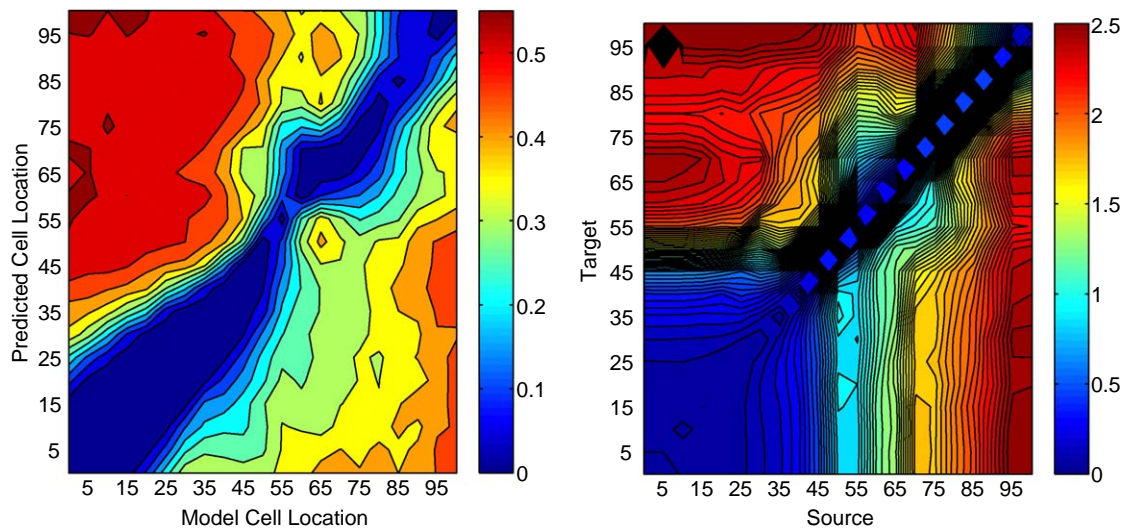


Fig. 6. Mutual prediction (left) and continuity (right) results based on delay coordinate reconstruction.

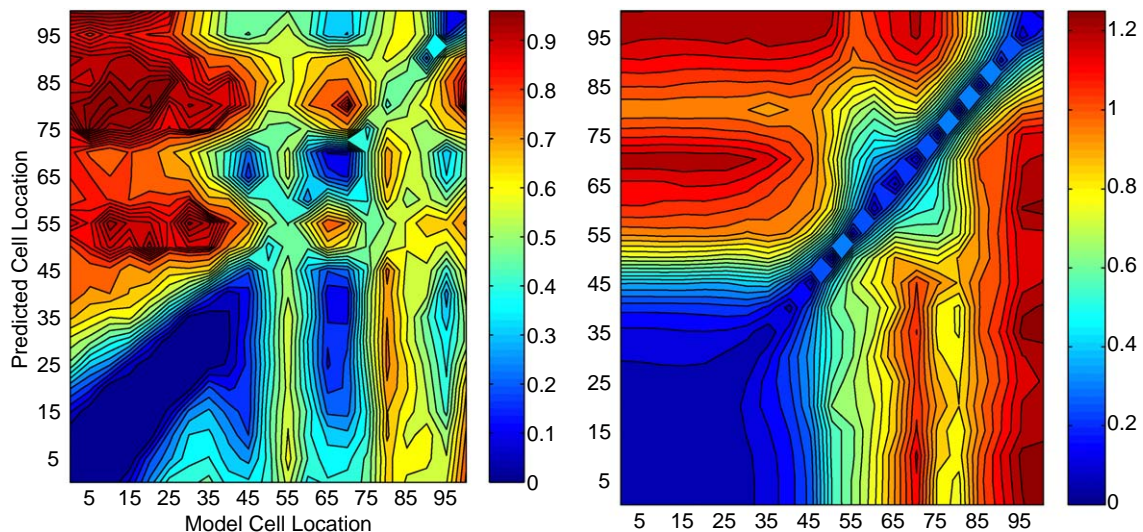


Fig. 7. Mutual prediction (left) and continuity (right) results using 1000 point time series.

measured variables comprising our attractor (10,000 points per dimension). By contrast, the delay coordinate approach “dilutes” the data in that we now have 10,000 points (only 1 time series) spread into three dimensions, giving 3333 data points per dimension. As a result the data have a greater spread and the average  $\varepsilon^*$  increases.

Mutual prediction suffers from this same effect. As before, there exists a clear asymmetry in the directionality of the predictions, that is, attractors reconstructed from lattice sites near  $x = 1$  do a better job at predicting those near  $x = 0$  than vice versa. However some of the detail is lost, for example, lattice sites near  $x = 65$  are no longer able to make accurate forecasts for the dynamics at other locations. The main point to make here is that much of the relevant dynamical information is contained in a single variable. While it is advantageous to form attractors using measurements of as many state variables as possible, pertinent information such as the asymmetry in population flow can be preserved with only a single measurement.

Another important question deals with the size of the data set under consideration. Even long time series of ecological data are limited to a few hundred or possibly 1000 points. In order to test the performance of these algorithms on limited data, the analysis was repeated using 1000 observations of the system dynamics. Attractors were again formed using both predator and prey variables and both continuity and mutual prediction algorithms were employed for the analysis. The results are shown in Fig. 7. Both sets of results clearly demonstrate an ability to detect the asymmetry in spatial information flow using both mutual prediction and continuity statistics. Due to the limited number of data the search radius for the mutual prediction algorithm was increased to  $\varepsilon = 0.05$ . Qualitatively few differences exist between these results and those obtained using 10,000 point time series. For this particular system, 1000 points are sufficient for populating the attractors such that the coupling between various spatial locations can still be observed. For shorter data sets the practitioner will likely have to alter the algorithms slightly. For example, the prediction error algorithm selects all points within a radius  $\varepsilon$  and makes the forecast assuming equal weighting ( $1/n_\varepsilon$ ) for all points. More intelligent weighting schemes have been proposed (Little et al., 1996) that may make better use of limited data. Another possibility is to make use of kernel density estimation techniques (see Silverman, 1986). Rather than simply counting points in an  $\varepsilon$ -ball, one may weight them according to their distance from the fiducial trajectory. Parametric or semi-parametric approaches may also prove useful when there exists some a priori knowledge of the distribution of the underlying populations. Drawing inferences about asymmetry from short and/or noisy time series may also require the use of surrogate data sets (Theiler et al., 1992). Metrics

computed from the population time series could be compared against those obtained for the surrogates (where no coupling exists) in order to better assess the significance of the result.

## 5. Conclusions

Both mutual prediction and the continuity statistics provided useful inferences about dynamical interdependence (coupling) for this spatially distributed predator–prey system. Cross-correlation also provided evidence of coupling, although we emphasize that cross-correlation is not guaranteed to perform well with nonlinear systems. Perhaps more important, mutual prediction and continuity clearly indicated the asymmetric flow of information and, thus, the directional nature of the coupling in this system with a spatial gradient. Cross-correlation provides no information about such asymmetries.

Asymmetric movement of animals is a topic of great interest in the study of spatial systems. For example, the concept of source–sink populations provides an extreme example of asymmetric movement in which source populations may contribute to sinks, but there is no movement in the opposite direction (Pulliam, 1988). Identification of sources and sinks is not only of theoretical interest but is very important to conservation. Sink habitat may show large abundances of animals at times, so abundance is not a reliable indicator of habitat quality (Horne, 1983). Additional information about coupling is needed to make informed decisions about relative efforts devoted to protection of different habitats. Models for the evolution of dispersal frequently predict different rates of movement (inducing coupling asymmetries) among population components with different suitabilities and abundances. Hypotheses and associated models of habitat selection predict asymmetric movement based on gradients among locations in expected fitness (Fretwell and Lucas, 1970; Fretwell, 1972; Nichols and Kendall, 1995).

As illustrated by our example of a predator–prey system, continuity and mutual prediction also should be useful in identifying asymmetries in the coupling of food web components. In fact, these metrics should be useful in distinguishing “top-down” and “bottom-up” population regulation (Harrison and Cappuccino, 1995; Turchin, 1995), as these concepts can be viewed as manifestations of asymmetric coupling. Indeed, consideration of the mechanisms underlying dynamical interdependence in ecological systems leads us to hypothesize that asymmetric coupling may be much more common in such systems than symmetric coupling. The continuity and mutual prediction algorithms described herein provide tools that permit investigation of this hypothesis using time-series data.

In addition to theoretical and conservation importance of asymmetries in dynamical interdependence, such asymmetries should be extremely relevant to the informed design of animal monitoring programs. One of the two central problems in the design of such programs involves sampling space in a manner that permits inference about locations that are not sampled (Yoccoz et al., 2001; Pollock et al., 2002). Because continuity and mutual information permit inference about asymmetries in the flow of information, they should permit informed selection of sample locations. For example, in large spatial systems with varying degrees of coupling among potential sample units, it should be possible to select units that are maximally informative about dynamics of either the entire system or specific system components.

Although both continuity and mutual prediction provide inference about asymmetric coupling, the two approaches do not yield identical inferences. Although coupling can be detected by both approaches, we suspect that continuity may be the approach of choice if the detection of dynamical interdependence is of primary interest. An alternative objective will be to use information from an observed system component to make predictions about another system component, or the same component at a future time, in which case the prediction metric may be utilized.

In summary, we believe that continuity and mutual prediction hold great promise for the study of complex ecological systems, but we note that additional work is still needed. In particular, the length of the time series necessary for these approaches to yield useful results requires further investigation. While we have demonstrated success using data sets as small as 1000 points, further refinements in the algorithms could extend their applicability to even shorter time series. In addition, sampling variation is nearly always associated with estimates of the state variables of ecological systems (e.g., Williams et al., 2002). The results reported in this paper are based on long time series without sampling variation (measurement error). The next step is to investigate shorter time series of estimates with measurement error in order to assess the limits to the utility of these methods for real-world ecological systems.

## Acknowledgments

We thank Stephen Ellner (Cornell University) for insightful comments on an early version of this paper.

## References

- Bjørnstad, O., Grenfell, B., 2001. Noisy clockwork: time series analysis of population fluctuations in animals. *Science* 293, 638–643.
- Bjørnstad, O., Ims, R., Lambin, X., 1999a. Spatial population dynamics: analyzing patterns and processes of population synchrony. *Trends Ecol. Evol.* 14, 427–432.
- Bjørnstad, O., Stenseth, N., Saitoh, T., 1999b. Synchrony and scaling in dynamics of voles and mice in northern Japan. *Ecology* 80, 622.
- Blums, P., Nichols, J., Lindberg, M., Hines, J., Mednis, A., 2003. Estimating breeding dispersal movement rates of adult female European ducks with multistate modeling. *J. Anim. Ecol.* 72, 292–307.
- Clobert, J., Danchin, E., Dhondt, A., Nichols, J., 2001. *Dispersal*. Oxford University Press, Oxford.
- Constantino, R., Cushing, J., Dennis, B., Desharnais, R., 1995. Experimentally induced transitions in the dynamic behaviour of insect populations. *Nature* 375, 227–230.
- Constantino, R.F., Desharnais, R.A., Cushing, J.M., Dennis, B., 1997. Chaotic dynamics in an insect population. *Science* 275, 389–391.
- Dennis, B., Desharnais, R., Cushing, J., Constantino, R., 1995. Nonlinear demographic dynamics: mathematical models, statistical methods, and biological experiments. *Ecol. Monogr.* 65, 261–281.
- Dennis, B., Desharnais, R., Cushing, J., Constantino, R., 1997. Transitions in population dynamics: equilibria to periodic cycles to aperiodic cycles. *J. Anim. Ecol.* 66, 704–729.
- Dieckmann, U., Law, R., Metz, J., 2000. *The Geometry of Ecological Interactions: Simplifying Spatial Complexity*. Cambridge University Press, Cambridge.
- Durrett, R., Levin, S., 1998. Spatial aspects of interspecific competition. *Theor. Popul. Biol.* 53, 30–43.
- Fraser, A.M., Swinney, H.L., 1986. Independent coordinates for strange attractors from mutual information. *Phys. Rev. A* 33, 1134–1140.
- Fretwell, S.D., 1972. *Populations in a Seasonal Environment*. Princeton University Press, Princeton, NJ.
- Fretwell, S.D., Lucas, H.L., 1970. On territorial behavior and other factors influencing habitat distribution in birds. i. theoretical development. *Acta Biotheor.* 19, 16–36.
- Harrison, S., Cappuccino, N., 1995. Using density-manipulation experiments to study population regulation. In: Cappuccino, N., Price, P.W. (Eds.), *Population Dynamics: New Approaches and Synthesis*. Academic Press, New York, pp. 131–147.
- Hastings, A., 2001. Transient dynamics and persistence of ecological systems. *Ecol. Lett.* 4, 215–220.
- Hastings, A., Hom, C., Ellner, S., Turchin, P., Godfray, H., 1993. Chaos in ecology: is mother nature a strange attractor? *Ann. Rev. Ecol. Syst.* 24, 1–33.
- Horne, B.V., 1983. Density as a misleading indicator of habitat quality. *J. Wildlife Manag.* 47, 893–901.
- Kantz, H., Schreiber, T., 1999. *Nonlinear Time Series Analysis*. Cambridge University Press, Cambridge.
- Karanth, K., Sunquist, M., 1995. Prey selection by tiger, leopard and dhole in tropical forests. *J. Anim. Ecol.* 64, 439–450.
- Keeling, M.J., Rohani, P., 2002. Estimating spatial coupling in epidemiological systems: a mechanistic approach. *Ecol. Lett.* 5, 20–29.
- Kennel, M.B., Brown, R., Abarbanel, H.D.I., 1992. Determining embedding dimension for phase-space reconstruction using a geometrical construction. *Phys. Rev. A* 45 (6), 3403–3411.
- Koenig, W., 1999. Spatial autocorrelation of ecological phenomena. *Trends Ecol. Evol.* 14, 22–26.
- Korpimäki, E., Krebs, C., 1996. Predation and population cycles of small mammals. *BioScience* 46, 754–764.
- Krebs, C., Boutin, S., Boonstra, R., Sinclair, A., Smith, J., Dale, M., Martin, K., Turkington, R., 1995. Impact of food and predation on the snowshoe hare cycle. *Science* 269, 1112–1115.
- Little, S., Ellner, S., Pascual, M., Neubert, M., Kaplan, D., Sauer, T., Caswell, H., Solow, A., 1996. Detecting nonlinear dynamics in

- spatio-temporal systems, examples from ecological models. *Physica D* 96, 321–333.
- Moniz, L., Pecora, L.M., Nichols, J.M., Todd, M.D., Wait, J.R., 2004. Dynamical assessment of structural damage using the continuity statistic. *Structural Health Monitoring* 3 (3), 199–212.
- Nichols, J.D., Kendall, W., 1995. The use of multistate capture–recapture models to address questions in evolutionary ecology. *J. Appl. Stat.* 22, 835–846.
- Ott, W., Yorke, J., 2003. Learning about reality from observation. *SIAM Online J. Dyn. Sys.* 2 (3), 297–322.
- Pascual, M., 1993. Diffusion-induced chaos in a spatial predator–prey system. *Proc. Roy. Soc. Lond. B* 251, 1–7.
- Pascual, M., Ellner, S., 2000. Linking ecological patterns to environmental forcing via nonlinear time series models. *Ecology* 81 (10), 2767–2780.
- Pascual, M., Levin, S.A., 1999. From individuals to population densities: searching for the intermediate scale of nontrivial determinism. *Ecology* 80 (7), 2225–2236.
- Pecora, L., Carroll, T., Heagy, J., 1995. Statistics for mathematical properties of maps between time-series embeddings. *Phys. Rev. E* 52 (4), 3420–3439.
- Pecora, L.M., Carroll, T.L., 1996. Discontinuous and nondifferentiable functions and dimension increase induced by filtering chaotic data. *CHAOS* 6 (3), 432–439.
- Pollock, K.H., Nichols, J.D., Simons, T.R., Farnsworth, G.L., Bailey, L., Sauer, J., 2002. Large scale wildlife monitoring studies: statistical methods for design and analysis. *Environmetrics* 13, 1–15.
- Post, E., Forchhammer, M.C., 2002. Synchronization of animal population dynamics by large-scale climate. *Nature* 420, 168–171.
- Pulliam, H.R., 1988. Sources, sinks, and population regulation. *Am. Nat.* 132, 652–661.
- Ranta, E., Kaitala, V., Lundberg, P., 1997. Population variability in space and time: the dynamics of synchronous population fluctuations. *Oikos* 83, 376–382.
- Rhodes, O., Chesser, R., Smith, M. (Eds.), 1996. *Population Dynamics in Ecological Space and Time*. University of Chicago Press, Chicago.
- Sauer, T., Yorke, J.A., Casdagli, M., 1991. Embedology. *J. Stat. Phys.* 65, 579.
- Schaffer, W., 1985. Order and chaos in ecological systems. *Ecology* 66, 93–106.
- Schaffer, W., Kot, M., 1986. Chaos in ecological systems: the coals that newcastle forgot. *Trends Ecol. Evol.* 1, 58–63.
- Schiff, S.J., So, P., Chang, T., Burke, R.E., Sauer, T., 1996. Detecting dynamical interdependence and generalized synchrony through mutual prediction in a neural ensemble. *Phys. Rev. E* 54 (6), 6708–6724.
- Silverman, B.W., 1986. *Density Estimation for Statistics and Data Analysis*. Chapman & Hall, London.
- Spendelov, J., Nichols, J., Nisbet, I., Hays, H., Cormons, G., Burger, J., Safina, C., Hines, J., Gochfeld, M., 1995. Estimating annual survival and movement rates within a metapopulation of roseate terns. *Ecology* 76, 2415–2428.
- Takens, F., 1981. Detecting strange attractors in turbulence. In: Rand, D., Young, L.-S. (Eds.), *Dynamical Systems and Turbulence*, Lecture Notes in Mathematics, vol. 898. Springer, New York, pp. 366–381.
- Theiler, J., Eubank, S., Longtin, A., Galdrikian, B., Farmer, J.D., 1992. Testing for nonlinearity in time-series—the method of surrogate data. *Physica D* 58 (1–4), 77–94.
- Tobin, P.C., Bjørnstad, O.N., 2003. Spatial dynamics and cross-correlation in a transient predator–prey system. *J. Anim. Ecol.* 72 (3), 46–467.
- Turchin, P., 1995. Population regulation: old arguments and a new synthesis. In: Cappuccino, N., Price, P.W. (Eds.), *Population Dynamics: New Approaches and Synthesis*. Academic Press, New York, pp. 19–40.
- Webster, M., Marra, P., Haig, S., Bensch, S., Holmes, R., 2002. Links between worlds: unraveling migratory connectivity. *Trends Ecol. Evol.* 17, 76–83.
- Whitney, H., 1936. Differentiable manifolds. *Ann. Math.* 37, 645.
- Williams, B.K., Nichols, J.D., Conroy, M., 2002. *Analysis and Management of Animal Populations*. Academic Press, San Diego.
- Williams, G.P., 1997. *Chaos Theory Tamed*. Joseph Henry Press, Washington, DC.
- Yoccoz, N.G., Nichols, J.D., Boulinier, T., 2001. Monitoring of biological diversity of biological diversity in space and time. *Trends Ecol. Evol.* 16, 446–453.